Measurement of liquid film distribution in near-horizontal pipes with an array of wire probes

P. Andreussi*, University of Pisa, Italy

E. Pitton, University of Udine, Italy

P. Ciandri, D. Picciaia, A. Vignali, TEA Sistemi spa, Italy

M. Margarone, ENI E&P, Italy

A. Scozzari, CNR-ISTI, Pisa, Italy

* Corresponding author. Present address: Department of Civil and Industrial Engineering, University of Pisa. Largo L. Lazzarino, 56100 Pisa, Italy.

Tel.: +39 050 639 6136; fax: +39 050 639 6110.

E-mail address: paolo.andreussi@tea-group.com.

Abstract

A test section consisting of a circumferential array of conductance probes has been developed to measure the thickness distribution around the pipe wall of a liquid layer flowing in near horizontal pipes. When the film thickness is known, the array can be employed to measure the local film flow rate by injecting a high conductivity tracer into the liquid flowing at pipe wall.

The test section consists of a short pipe made of a non-conducting material installed in a flow rig designed to operate at an appreciable pressure (40 Bar). The flow loop is made of metallic pipes connected to the electrical earth. The conductance probes are made of three parallel, rigid wires spaced along the flow direction and are used to measure the height or the electrical conductivity of the liquid layer. The three-electrode geometry is aimed at minimizing current losses toward earth. The simultaneous operation of all the probes of the array, without multiplexing, allows a substantial reduction of current dispersion and a good circumferential resolution of film thickness or conductivity measurements. The probe geometry may generate an appreciable disturbance to the gas-liquid interface. This aspect of the proposed method has been studied with an experimental and numerical investigation relative to free falling liquid layers.

1. INTRODUCTION

Pipeline transportation over long distances of natural gas or saturated steam in presence of a liquid phase is a common practice in the oil and in the geothermal industry and can be extremely challenging when major flow assurance issues, such as solid formation and deposition or pipe wall corrosion, arise. In near-horizontal pipes, stratified flow conditions are encountered at moderate phase velocities. At higher gas velocity, only part of the liquid flows at the pipe wall, while the remaining liquid is entrained by the gas in the form of droplets which tend to deposit back onto the wall layer. The competing phenomena of droplet entrainment and deposition determine the liquid holdup, which is the fraction of the pipe cross-section occupied by the liquid phase. The resulting flow pattern is usually classified as stratified-dispersed flow.

In one-dimensional gas-liquid flow models (see for instance [1]), stratified and stratified-dispersed flow in inclined pipes and annular flow in a vertical pipe are described by the same set of conservation equations. The closure equations required for these two regimes are quite different, due to the different effects of gravity, but while the data and correlations relative to vertical annular flow are abundant, there are almost no correlations for horizontal or inclined flow and very few data are available for the development or validation of flow models. The main objective of the present work is the development of a new experimental method able to provide these data.

The critical flow parameters to be measured in stratified-dispersed flow are the flow rate and the circumferential thickness distribution of the liquid layer flowing at pipe wall. This is because these parameters determine the overall liquid hold-up in the pipe and the value of the frictional pressure losses. Besides to the fluid dynamic issue, a better knowledge of the flow behavior of the wall layer has a wide number of implications in heat transfer and flow assurance studies.

Many authors measured the liquid film thickness by determining the electrical conductance between either two parallel wires or two flush-mounted electrodes. Wire probes have been introduced by Miya et al. [2] and studied in details by Brown et al. [3]. Flush-mounted probes have been first described by Coney [4]. The two-ring probe is a particular type of flush-mounted probe and has been used to measure the mean thickness of liquid films flowing in a vertical pipe [5]. Among the numerous applications of conductance probes, the work by Geraci et al. [6] is significant because these authors used both wire and flush-mounted probes for the measurement of the circumferential liquid film thickness distribution in stratified-dispersed flow. Multiple ring probes have been used to study slug flow in inclined pipes [7]. Zhao et al. [8] used a set of four flush-mounted probes to study the flow of large disturbance waves in a vertical film. The electrical behavior and the application of ring probes to other flow patterns has been described in details by Andreussi et al. [9] and Fossa [10]. Barral and Angeli [11] studied the fine interfacial structure of water-oil flow in a horizontal pipe with two double-wire conductance probes. These authors report that the disturbances generated by these probes on liquid flow are negligible.

Along with the development of multiple probe test sections, advanced conductance methods have also been proposed, such as the wire mesh sensor (WMS) [12]. This technique provided good results when studying bubble or slug flow and, in a recent paper, Vieira et al. [13] adopted a WMS to study stratified-dispersed flow in a horizontal pipe. As stated by these authors, they were not able to detect thin liquid films flowing in the upper part of the pipe. Therefore, in their experiments the crossing points of the WMS closer to the wall than 1 mm were disregarded. The case of thin films has been faced by Damsohn and Prasser [14] with the development of a sensor based on the wire mesh approach for the analysis of the electrical signals generated by a matrix of flush-mounted electrodes.

This sensor is characterized by high time and spatial resolution, but its use is limited by the saturation of the electrical response at increasing the film thickness. According to these authors, the maximum film thickness that can be measured with their sensor is 0.8 mm. The measuring range of flush-mounted electrodes has been extended by Tiwari et al. [15], who developed a test section of flush-mounted electrodes spaced at different distances among them. With this set-up, the maximum film height which was possible to measure, with an acceptable accuracy, was equal to 3.5 mm. This value still appears to be unsatisfactory when studying stratified flow in a horizontal pipe in presence of large disturbance waves, whose height can largely exceed 3.5 mm [16]. In principle, the limiting value of the film height reported by Tiwari et al. [15] can be extended by increasing the distance between the electrodes. This requires the simultaneous acquisition of signals generated by sensors operating in different height ranges.

The liquid film thickness in annular or stratified flows has also been measured with other techniques. Some of these methods, such as the γ-ray or the X-ray tomography [17-18], the Laser Induced Fluorescence [19] or other optical methods can be quite expensive. However, the main reason to disregard these methods for the present application is that it may be difficult to use the same method to measure both the film thickness and the concentration of an appropriate tracer.

In the present work, a conductance method based on the use of an array of non-conventional wire probes has been developed to measure the local thickness or the conductivity of a liquid layer flowing at pipe wall. In general, the conductivity of a liquid can be modified by increasing its salinity and, at low salinity, the conductivity is proportional to the salt concentration. When the film thickness is known, a salt solution can be used as a tracer to measure the flow rate of a liquid film by continuously adding the solution to the film and measuring the liquid conductivity. The smooth injection of a very small tracer flow rate does not modify the film flow characteristics or alter the linear relation between liquid conductivity and salt concentration. In order to perform this type of measurements, the film thickness distribution around the pipe wall can be measured in the absence of tracer injection, while the local film flow rate can be derived from the variation of the probe conductance when the tracer inlet flow is switched on. Alternatively, two consecutive probe arrays, with tracer injection between the arrays, can be used to perform simultaneous measurements of the local film thickness (with the first array) and flow rate (with the second).

Tracer injection experiments can be performed both under developing or fully developed flow conditions and, in developed flow, the tracer method can be used to measure also the rate of droplet exchange between the wall layer and the gas core for vertical annular flow [20-21]. To this purpose, it is necessary to measure the tracer concentration in the liquid film at a number of locations along the pipe. These measurements can be made with a set of conductance probes, combining film thickness and conductivity measurements [22]. Recently, the complex application of the tracer method to stratified-dispersed flow in a horizontal pipe has been reported by Pitton et al. [23]. The combined use of the tracer injection system and the measuring sections described in the present paper allowed these authors to measure the local film flow rate and the rates of liquid exchange between the wall layer and the gas core.

The range of liquid thicknesses that we expect to measure in an 80 mm pipe goes from a minimum of 0.05 mm to a maximum of 50-60 mm. Having this objective in mind, wire probes appear to be a better choice than flush-mounted probes, due to their intrinsic linearity, which allows the height of both thin and thick liquid layers to be measured with good accuracy. The expected measuring range of the proposed test section is very wide, but it can easily be attained using the same electronics by

properly choosing the liquid conductivity. This represents a major advantage of wire probes when compared with flush-mounted probes or other methods adopted in the literature to measure the thickness of a liquid layer.

The main disadvantage of wire probes is that they are intrusive. The same problem arises with WMS and recently a study on the intrusiveness of a three layer WMS has been presented by Ito et al. [24]. These authors observed an appreciable effect of the wire mesh on the velocity of gas bubbles crossing the mesh. This flow condition is quite different from the case of film flow, but the work of Ito et al. [24] represents a serious warning against the use of intrusive probes. This potential limitation of wire probes is examined into details in the present paper, with a careful computation of the flow and the electrical fields around the electrodes.

The conductance probes proposed in the present work are made of three rigid wires spaced along the flow direction. A circumferential array of such probes is installed in a test section made of a non-conducting material which is part of a flow rig designed to operate at an appreciable pressure, composed of metallic pipes electrically connected to the earth potential. A common excitation signal is fed to all the central electrodes (transmitting electrodes) of the array, while the external electrodes (receiving electrodes) are actively kept at the same, earth potential. This allows to minimize current losses towards earth and to mitigate possible interferences between adjacent probes. The simultaneous operation of all the probes of the array, without multiplexing, is also useful to obtain a good circumferential resolution of film thickness or conductivity measurements.

A three electrode geometry of conductance probes has been used by other authors. For instance, Kim et al. [25] developed a three electrode flush-mounted probe to compensate the temperature effects on thickness measurements. A three layer wire mesh has been developed by Richter et al. [26] to measure the velocity of the gas bubbles crossing the mesh. In both cases, the objectives of these authors were substantially different from those of the present method.

2. CONDUCTANCE PROBES

2.1 Basic Theory

Brown et al. [3] showed that the impedance between two electrodes immersed in a conducting liquid is mainly resistive and does not depend on the frequency of the signal applied to the electrodes when this frequency is high enough to make double-layer effects negligible. In this case, the electrical potential generated around the electrodes can be computed by integrating Laplace equation:

$$\nabla^2 \phi = 0 \qquad \text{on } \Omega \tag{1}$$

$$\phi = \phi_0 \qquad \text{on } \partial\Omega \ ,$$

where ϕ is the electrical potential, Ω the domain, $\partial\Omega$ the domain boundary and ϕ_0 the value that the potential assumes at the boundary. Once the spatial distribution of the electrical potential has been determined, it is possible to calculate the electrical current density vector, $\vec{J}$, with the following relationship:

$$\vec{J} = -\gamma \cdot \nabla \phi, \tag{2}$$

where γ is the electric conductivity of the medium. The conductance between the electrodes can be derived as the ratio between the current and the potential difference.

The main advantage of wire probes is that the conductance between the electrodes, G, is a linear function of the film height, h, and the liquid conductivity, γ ,

$$G = k \cdot \gamma \cdot h, \tag{3}$$

where k is a constant related to the probe geometry. Brown et al. [3] have shown that at increasing frequency of the applied electrical signal, k, tends to the value:

$$k = \frac{\pi}{\ln\left[(d-r)/r\right]}, \tag{4}$$

where r is the radius of the wires and d is the distance between them. For a non-conducting liquid, Brown et al. [3] showed that similar equations hold for the capacitance between the electrodes, with the dielectric constant replacing the conductivity in Eq. (3).

The present flow rig has been designed to operate at significant pressure (the design pressure is 40 Bar). This level of pressure can be easily sustained by the non-conducting sections of the pipe used to install the conductance probes. However, these sections are part of a metallic rig connected to the electrical earth and this may represent a threat to the integrity of the probe signals. This potential limitation of the experimental method has been faced by adopting a novel probe geometry which consists of three rigid wire electrodes spaced along the flow direction. In these probes the central electrode is set at a given potential and the two side electrodes are actively set at the same reference potential of the metallic pipe. In practice, with this probe configuration the side electrodes act as screens to current dispersion towards the metallic pipe.

For an unbounded liquid film the conductance of a three wire probe can be theoretically derived from Laplace equation. In this case the constant k assumes the value

$$k = \frac{4\pi}{3\ln\left[(d-r)/r\right] - \ln\left[(2d-r)/(d+r)\right]}. \tag{5}$$

This equation allows the probe and the related electronics to be properly designed when the probe is installed in an insulated pipe. When d and r are assigned, a comparison between Eqs. (4) and (5) shows that with two receiving electrodes the current signal increases by about 40%. The other advantages related to the three-electrode configuration and the use of an array of conductance probes, operating without multiplexing, are discussed in the next section.

2.2 Estimation of current dispersion

The conductance measurement between wire electrodes can be significantly altered by the presence of nearby probes and/or side currents directed towards the metallic sections of the pipe set at the earth potential. The probe conductance and the side currents can be derived from the numerical integration of Laplace equation with the appropriate boundary conditions. In the following examples, this integration has been performed for the probe geometry (electrode diameter and distance between the transmitting and receiving electrodes) reported in Section 2.3.

In Fig. 1, the electrical field relative to a single three-wire probe immersed in a liquid film of constant height is compared with the case of a two-wire probe. In these computations, the film height is equal to 8 mm and the distance between the terminal sections of the liquid film (connected to earth) and the

film width are both equal to 314 mm. From this figure, the difference between the two electrical fields can be detected at least from a qualitative point of view.

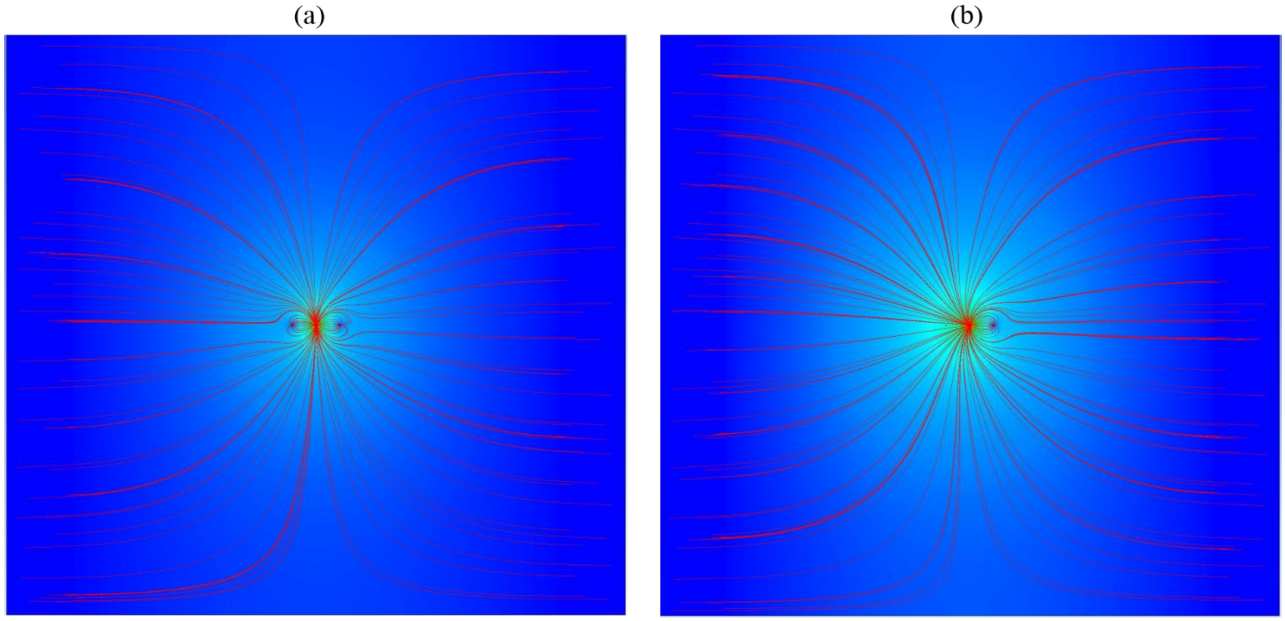

Fig. 1. Electrical fields of single three-wire probe (a) and two-wire probe (b) immersed in a liquid film of constant thickness.

In Fig. 2(a), the electrical field relative to an array of three-electrode probes spaced at a distance of 13.8 mm is shown. As can be seen from this figure, the side probes bound the electrical field of all the probes of the array into a restricted volume of liquid. A comparison with the case of a single three-electrode probe shown in Fig. 1(a) is useful to understand the effect of side probes. A similar evaluation is made in Fig. 2(b) for a two-electrode probe. Fig. 2 clearly shows the significant contribution of the active adjacent probes to the confinement of the electrical field of all the probes.

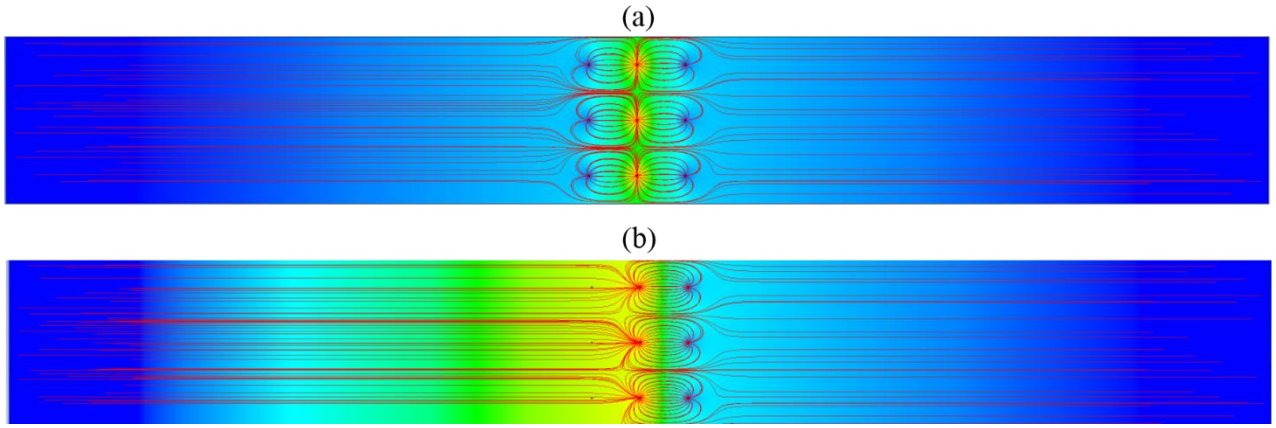

Fig. 2. Electrical fields of three-wire probe (a) and two-wire probe array (b) immersed in a liquid film of constant thickness

In Table A, the current dispersion expressed as fraction of the total current transmitted by the central electrode to the terminal sections of the liquid film is reported. As can be seen from this table, in both cases the current dispersion is relevant, though it is significantly smaller for the three-electrode probe.

Table A. Fractions of current dispersed to earth

	Three electrodes	Two electrodes
Single Probe	0.40	0.61
Probe Array	0.05	0.16

In this case, the fraction of current dispersion decreases from 0.4 for a single probe to 0.05 for a probe array. For a two-wire probe the dispersion decreases from 0.61 to 0.16. As can be seen from Table A, the effect of side probes is relevant and, in particular, a three-electrode array, without multiplexing, is able to minimize the current dispersion to earth. This explains why this probe configuration has been chosen.

The case of stratified flow in a circular pipe is considered in Fig. 3, where the current dispersion is plotted vs the dimensionless liquid height, h/D, for three and two-electrode arrays. The geometry of the system is described in Section 2.3. As can be seen from Fig. 3, for a three-electrode array, the current dispersion is approximately constant and about equal to 4% in the range $0 < h/D < 0.3$. This value rises to about 15% for a two-electrode array.

A careful probe calibration may account for the current dispersion towards the flanges when the height of the liquid layer does not significantly change with time or along the pipe, but the signal would be distorted when large waves or liquid slugs pass through the test section. In order to clarify this point, the simple case of a square wave crossing the test section is considered. In this example, the square wave ranges from a base value $h/D = 0.1$ to the value $h/D = 0.25$. In Fig. 4, the dimensionless conductance of the central probe derived from the numerical integration of Laplace equation is plotted as a function of the wave position along the test section. The conductance is normalized with respect to the value at $h/D = 0.25$. In this figure the readings relative to three or two-wire probes are compared. As can be seen from Fig. 4, the current dispersion significantly affects the reading of the two-wire probe, deforming the wave shape in particular on the side not screened by the receiving electrodes. The measurement of the three-wire probe is more localized, and the only deviation from the actual wave shape occurs when the wave crosses the probe. This deviation is due to the distance between the wires along the flow direction. This aspect of the probe geometry represents a potential limitation of the present measuring system. However, considering that the transit time of a wave or a liquid slug passing through the probes is of the order of 0.01 s, and the sampling frequency of the present measuring system is typically less than 100 s^{-1}, it is clear that this is a minor problem.

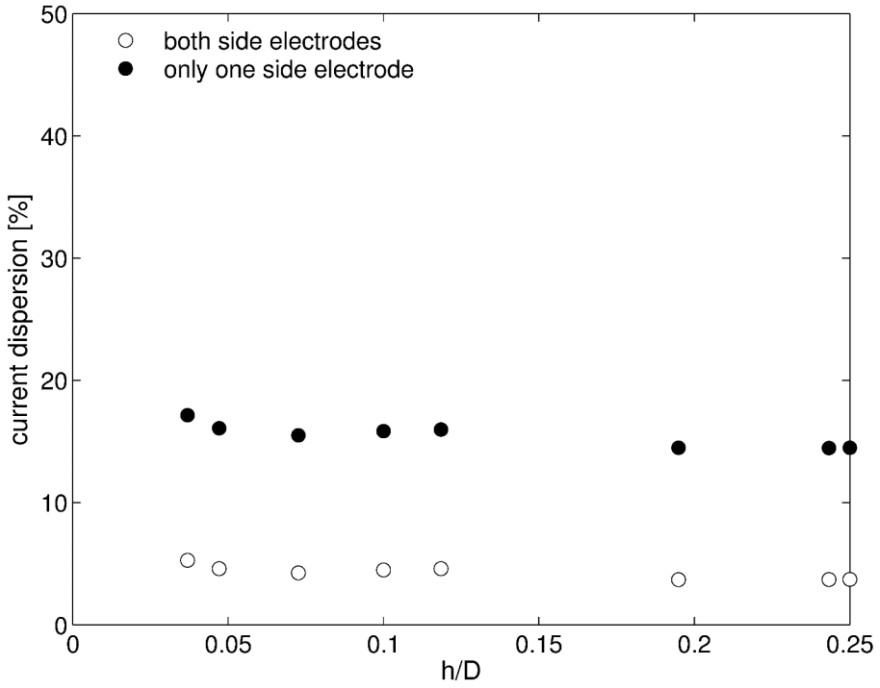

Fig. 3. Fraction of the electrical current going to the conducting pipe sections obtained by numerical simulations. Wire probe in stratified condition.

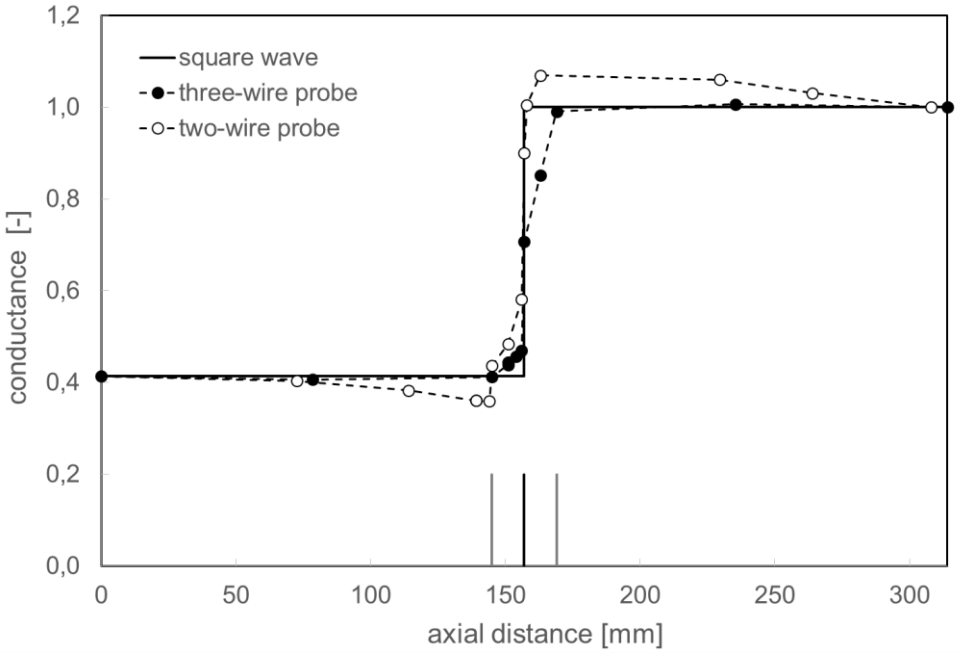

Fig. 4. Dimensionless conductance of the vertical probe as a function of a square wave position crossing the test section. In the two-wire configuration the receiving electrode not active is that on the right.

2.3 Wire probes

Fig. 5 shows the wire probe section developed for the present work. From this figure it can be seen that the test section consists of three arrays of 15 wire electrodes installed on three planes normal to the axis of the tube. For clarity, in Fig. 6 also a 3-D view of probes 1 and 2 (vertical and first lateral probe) of the test section is shown. Each probe consists of three parallel, stainless steel, rigid wires, 0.3 mm in diameter, aligned along the flow direction. The spacing along the flow direction between the wires is equal to 12 mm. With reference to Fig. 5, the short vertical wire (Probe 1) can be replaced with cross-sectional wire.

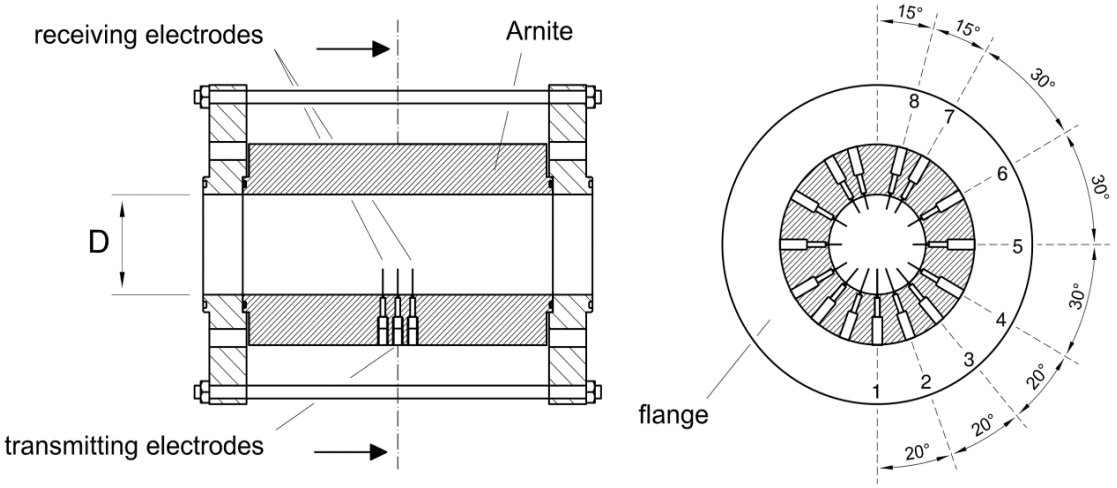

Fig. 5. Test sections developed in the present work.

The body of each measuring section is made of a PET plastic (Arnite), which is characterized by good mechanical properties, an excellent resistance to chemical agents and a maximum operating temperature equal to 120°C. Each measuring section is connected to the rest of the pipe with stainless steel flanges set at the earth potential. This allows the test section to be employed at appreciable pressure. O-ring static seals have been used in order to avoid liquid leaks between the main body of the measuring section and the stainless steel rods that support the wires.

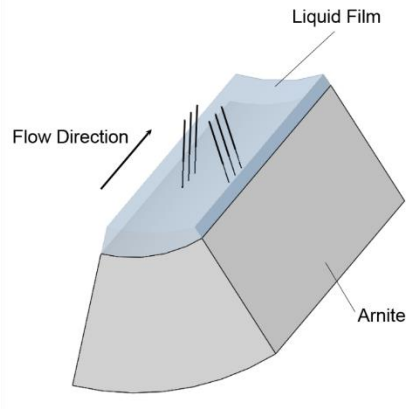

Fig. 6. Three dimensional view of the vertical and first lateral probes.

The overall experimental set-up consists of 6 measuring sections similar to that shown in Fig. 5. The distance among the measuring sections can be varied by means of a set of spacers. One of the possible configurations of the system is shown in Fig. 7, where also a ring probe section is shown. The set of measuring sections can also be used to study transient or developing flow conditions, such as the motion of interfacial waves, liquid slugs or elongated gas bubbles.

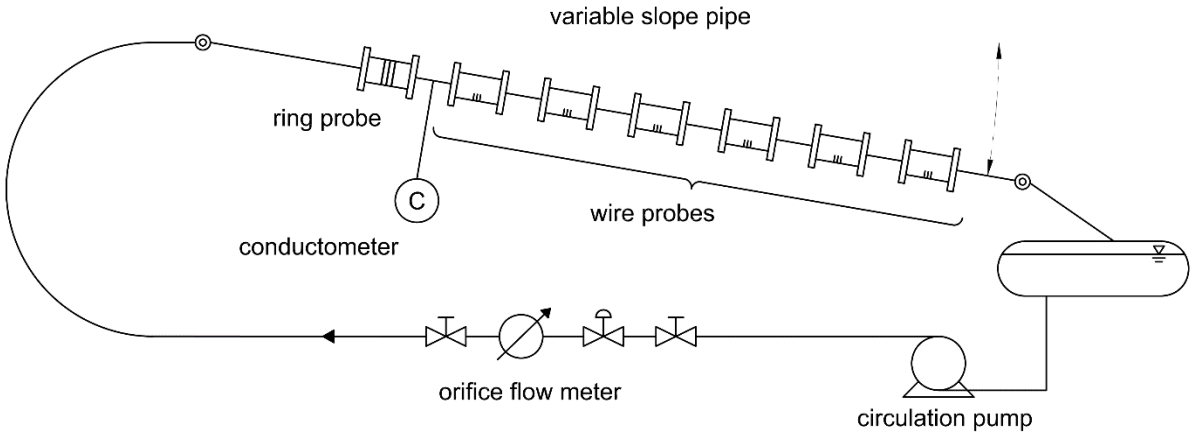

Fig. 7. Simplified chart of the flow loop used in present experiments.

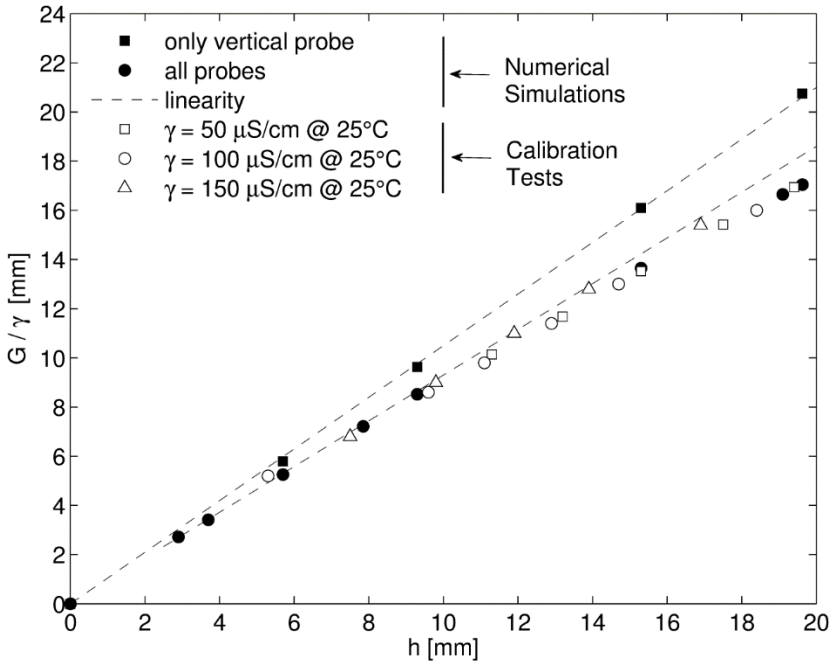

Fig. 8. Response of the vertical probe in stratified condition. Comparison between numerical simulations and calibration tests.

In a measuring section, the linearity of each probe is conserved also in presence of nearby probes and terminal flanges. This can be seen from Fig. 8, which reports the electrical response of the central probe computed by the numerical integration of Laplace equation for the two cases: a) only the

vertical probe is active, b) all probes are active. As can be seen from this figure, the presence of nearby probes alters the electrical response of the vertical probe. Nonetheless this probe maintains a linear behaviour up to film heights of 10 mm. Above this height the linearity slightly decays and a more careful probe calibration is required. An example of probe calibration is reported in the same figure, for three different values of the liquid conductivity. As can be seen from this figure, the calibration tests agree quite well with the numerical predictions, with a scatter of less than ±2%. Also for the inclined probes, the conductance is a linear function of the wetted length of the probe, which, for the present probe geometry and in stratified or annular flow, is equal for all the electrodes of the same probe.

2.4 Probe calibration

In practical applications, probe calibration is used to derive the relation between the liquid height and the measured conductance, while the theoretical computations are mainly used in order to design the probes and optimize their geometry. The static calibration of a probe can be performed by closing both ends of the non-conducting duct where the probe is installed with blind flanges and filling it with known volumes of liquid, thus simulating stratified flow conditions. In the calibration tests, the flanges are metallic and connected to earth in order to take into account the current dispersion. The liquid conductivity and temperature are carefully monitored. The results obtained with this method can be checked with the direct measurement of the liquid height performed with a micrometric head. This instrument is equipped with a thin needle, which allows an electrical loop to be closed when the needle tip touches the liquid surface. In successive validation tests the two methods agreed with a typical scatter of less than 0.1 mm and no systematic error was noticed.

When all measuring sections are installed in the main pipe, the micrometric head is used to measure the film height at various positions along the pipe. The objective of these measurements is to check probe calibrations and to verify if all measuring sections are aligned in the horizontal position. This is done by closing the outlet valve of the pipe, which is then filled with controlled volumes of liquid.

2.5 Effect of wires on liquid flow

Three-wire probes guarantee a good circumferential resolution of the measurements because the probes are aligned along the flow direction and the electrical field generated by each probe is bound by nearby probes into a restricted volume. However, they are more intrusive than conventional probes, considering the presence of three electrodes rather than two. This potential limitation of the probes deserves some attention.

The issue of flow disturbances induced by wire electrodes presents two distinct aspects: on one hand, the electrodes and in particular three arrays of 15 electrodes may modify the flow structure of the liquid layer. In order to limit this effect, the construction of the measuring sections allows single probes to be easily removed, when necessary. For instance, a three wire probe can be transformed into a two wire, accepting an increase of current dispersion toward the metallic pipe, or all the probes installed on the upper pipe wall can be removed when the liquid deposition on the upper wall is negligible.

On the other hand, the disturbances generated by the probes may alter the probe signal, thus causing an error in the film height readings. This effect has been analyzed by determining the flow field of

the liquid phase around the probe. To this objective, the Volume of Fluid model of a 3-D flow simulator (Ansys Fluent) has been used to determine the flow field around a three wire probe immersed in a falling film 10 mm high. The average velocity of the liquid around the probe is equal to 0.94 m/s. The results obtained are shown in Fig. 9, where both the side and front views of the gas-liquid interface are represented. As can be seen from this figure, the modifications of the interface around the wires are of the order of the wire diameter (0.3 mm) and increase in size going from the first electrode to the last.

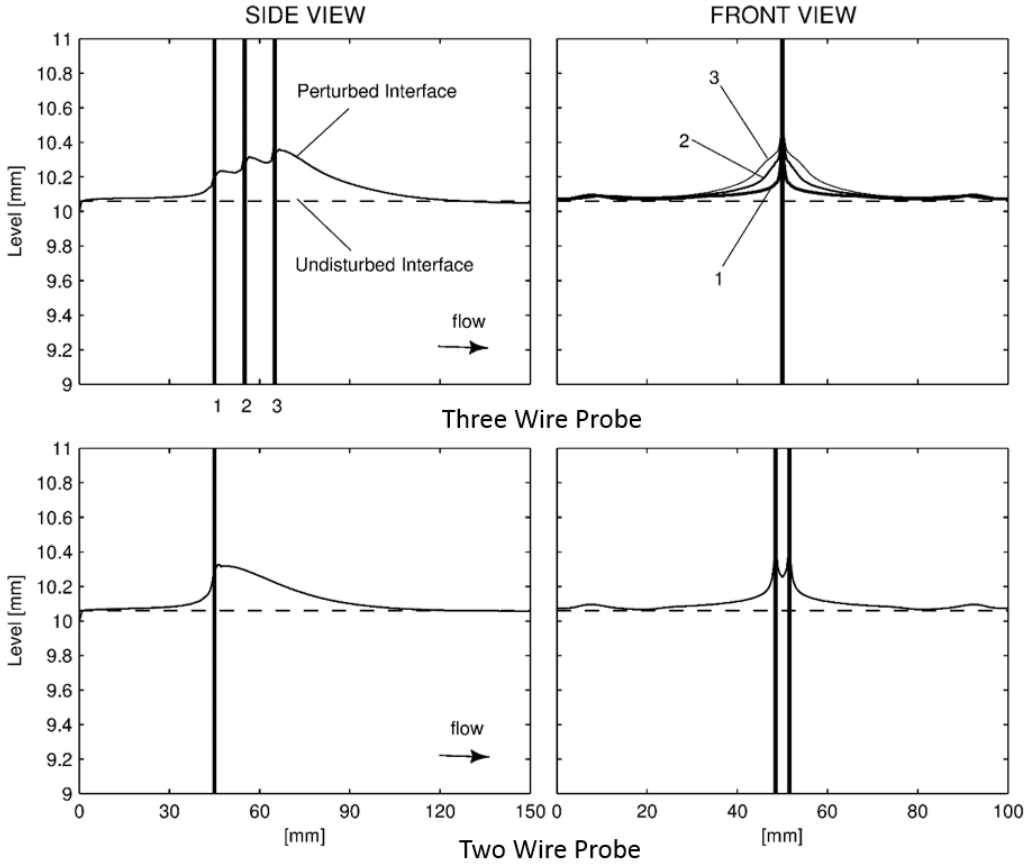

Fig. 9. Side and front view of the perturbed gas-liquid interface in presence of wire probes.

The overall effect of the flow disturbance caused by the electrodes on the probe conductance can be determined by solving the Laplace equation for the distorted shape of the gas-liquid interface. The result obtained for the case considered in Fig. 9 is an increase of the probe signal equal to 2.3% of the original, undisturbed signal. This value is significant because this potential source of error should be added to the others, such as the error associated with probe calibration, the measurement of the liquid conductance or the measurement of pipe inclination.

As shown in Fig. 9, the effect of wire-flow interactions is also significant for a conventional probe made of two 0.3 mm wires normal to the flow direction and spaced 3 mm apart. This distance appears to be the correct choice when a good circumferential resolution is required. The error caused by the flow disturbance for this conventional probe is smaller (1.8%), but, in practice, quite similar to the three wire case. It may be concluded that the problem of wire-flow interactions exists, but it is not specific of the probe configuration proposed in this work. To this it may be added that the use of wire

electrodes to determine the increase of liquid conductivity due to the injection of a tracer, once the film height has been measured, is exempt from this type of error.

2.6 Ring probe

Andreussi et al. [9] showed that the conductance between two ring electrodes is a linear function of the hold-up of the continuous liquid phase when the distance between the electrodes is larger than about two pipe diameters, independently on the shape of the wall layer. For shorter distances, these authors extended the theoretical solution determined by Coney [4] for flush-mounted, rectangular electrodes to ring electrodes. Devia and Fossa [27] found a very good agreement between their numerical solution of the Laplace equation and the simplified model proposed by Andreussi et al. [9].

In the present work, a ring probe has been used along with the wire probes to measure the hold-up of falling liquid films in near-horizontal pipes. This allows the effect of wire probe intrusiveness to be verified. In order to screen the probe from the metallic sections of the pipe, a three ring probe has been adopted. The probe is made of three 4 mm stainless steel rings spaced 40 mm apart. The body of the probe has been built with the same plastic material as the wire probes. The relatively short distance between the rings limits the measurement range of the probe at which the conductance is a linear function of the liquid holdup.

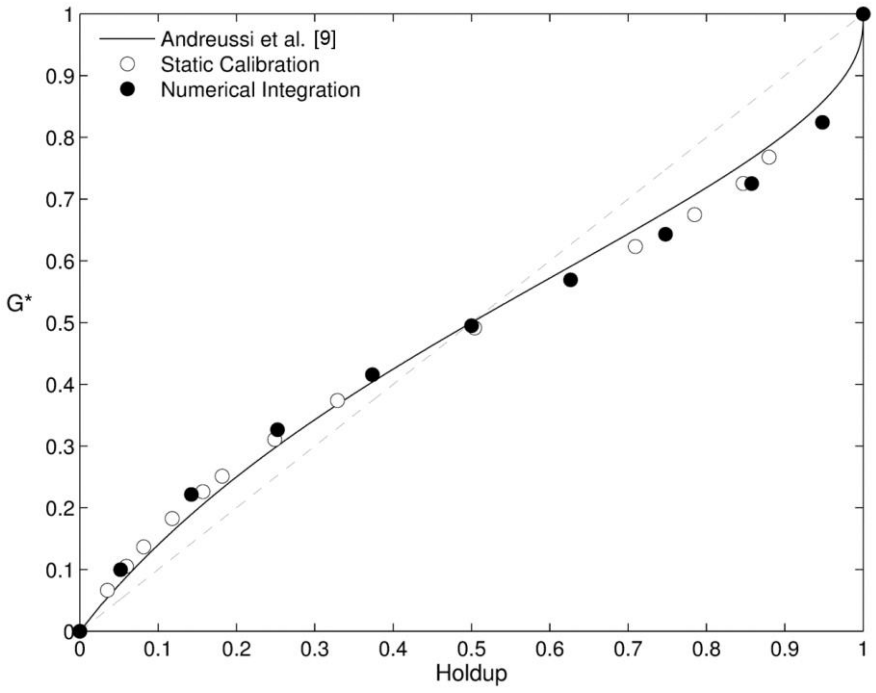

Fig. 10. Static calibration and numerical integration for a three ring probe compared with the theoretical model of Andreussi et al. [9].

In Fig. 10 the theoretical value of the dimensionless conductance G* obtained by the numerical integration of Laplace equation for the present geometry of the ring probe is compared with the results of the static calibration. In this figure the dimensionless conductance G* is the conductance normalized with respect to the conductance value for liquid holdup equal to 1. As can be seen from

this figure, the agreement between the numerical computations and the results of probe calibration is excellent. In the same figure also the predictions of the simplified model of Andreussi et al. [9] are reported. In this case the agreement between data and predictions is not as good. This may depend on different reasons, such as the different probe configuration, with three electrodes rather than two and the signal distortion due to the flanges connected to the earth potential.

3. ARCHITECTURE OF THE MEASUREMENT SYSTEM

Up to six measurement sections can be installed in the test rig. A measurement section consists of the following components:

- One array of wire probes, each consisting of three rigid wires aligned along the flow direction.
- The analog front-end connected to the relative probes.
- The local data acquisition system, which collects the signals originated by the front-end.

The number of voltage signals produced by the whole system can be as large as 90 at a maximum sampling frequency of 100 Hz per signal. In order to deal with these data, a workstation acts as data logger and interface to the human operator (HMI). A simplified block diagram, giving a general view of the whole measurement system is shown in Fig. 11.

For each measuring section, the array of 15 wire probes can be seen as a matrix made of three arrays of electrodes. The signals fed to the three arrays are handled as follows:

- A common excitation signal equal to 1.0 V is fed to all the electrodes of the central array. Such signal is in the form of an alternated voltage signal.
- The two external electrodes are connected in pairs and are actively set to the same potential of the earthed pipe, which corresponds to the zero voltage level of the excitation signal.
- All the other conductive surfaces of the experimental set-up (flanges, etc.) are also tied to the same potential, which is treated as a voltage reference.
- The observable parameter is the total current flowing into each pair of electrodes belonging to the external arrays, by closing the current loop of the excitation signal.

The reference potential can be considered as a "virtual earth", actively generated by a particular configuration of the analog front-end, which sources or sinks current in order to tie the potential of the controlled node (one side electrode) to a pre-determined value. This configuration permits to keep the two external arrays in a substantially equipotential plane, thus minimising the signal dispersion due to the external conductive components of the flow loop (because tied at the same potential of the electrodes) and probe-to-probe cross-talk (because adjacent electrodes belonging to the same array are actively forced to adhere to the same potential).

This configuration enables the simultaneous operation of the 15 measurement probes without multiplexing, thanks to the substantial absence of cross-talk between the different probes. The absence of multiplexing represents a noticeable advantage of the present set-up as it enhances signal integrity in the signal processing chain and binds the signals generated by the central array of electrodes into a limited volume of the liquid layer, due to the presence of nearby active electrodes. This feature of the system allows a more localized conductance measurement to be obtained and significantly limits current dispersion to earth.

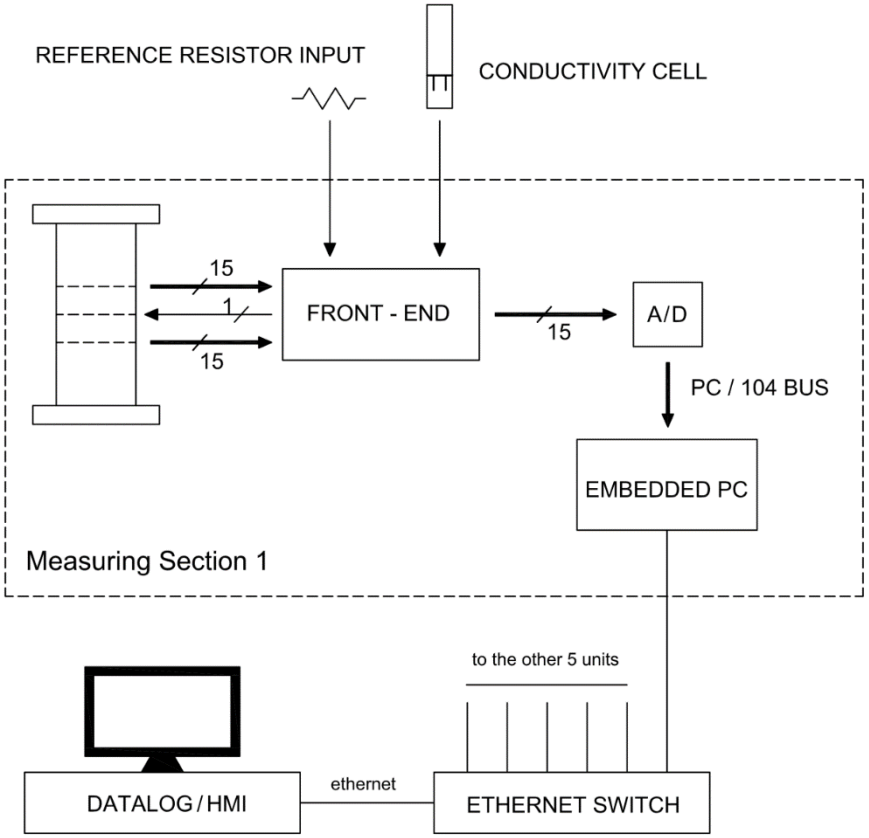

Fig. 11. Simplified block diagram of the measuring system.

3.1 Electronic circuit

The electronics of the sensor units (i.e., the analog front-end and the data conversion devices that interface the workstation with the analog signals) has been conceived and developed specifically for this application. Each sensor unit has a front-end and data conversion electronics mounted locally. The excitation signal supplied to the central array of electrodes (transmitting electrodes) is generated by a low distortion sinusoidal oscillator, set to a frequency of 100 kHz. Each front-end board is provided with a dedicated oscillator, and has the option to use an external source, e.g., a digital synthesis generator shared by all the measuring sections.

The two external arrays (receiving electrodes) are connected to dedicated wideband current-input circuits (trans-impedance amplifiers), followed by a demodulation stage, which performs simultaneous conversions of all the channels by an array of coherent demodulators, thus providing a rectified output after cutting-off the residual ripple. The 100 kHz working frequency has been chosen as a trade-off between high frequency needs (to cut-off demodulation ripple and make double layer effect negligible) and low frequency requirement (to limit the impact of jitter and switching noise of demodulators on the rectified output).

As specified in the previous section, this configuration does not require the use of a multiplexed scheme, with relevant advantages in terms of noise reduction and response to transients. In fact, such current-input stages tie their input potential to the reference potential of the whole electronic front-end, assuming the ideal Operational-Amplifier approximation and applying the virtual short circuit

principle as a consequence. As mentioned above, such reference potential corresponds also to the "zero" voltage level of the excitation signal, and is tied to the earth potential. In addition to that, as this equipotential array of current-input electrodes can be placed at the same potential of the other conductive wet surfaces of the experimental set-up, the unwanted currents flowing between each probe and the rest of the test apparatus can be limited. Moreover, since the excitation source generates a zero-averaged symmetrical and alternating signal, there is no DC component across any electrodes or across different probes that can potentially produce unwanted electrolytic effects. It must be noted that all the electrodes of the transmitting array are fed by in-phase signals having the same amplitude, thus further eliminating residual currents between the electrodes.

Fig. 12 presents the simplified structure of a measurement channel belonging to the analog front-end. The current signals coming from each pair of receiving electrodes are handled by a signal processing chain, which consists of the following stages: i) current to voltage conversion, ii) band-pass filter, iii) synchronous demodulation, iv) low-pass filter. Signals are then forwarded to the Analog to Digital (A/D) converter, a 16 bits, 16 channels, 200 ksamples/second A/D board, based on the industry-standard PC/104 bus. Such board is directly interfaced with a local controller, a SBC (Single Board Computer embedded PC), which buffers the data, performs further digital filtering, and handles the communication with the datalog/HMI (Human to Machine Interface) workstation, where the operator can control how the experiment evolves in real-time. The workstation also performs proper logging of all the collected data during each experiment. The local A/D conversion, which is performed in each sensor unit, permits to transmit all the acquired information in digital form, avoiding the transmission of analog signals over relatively long lines, which are prone to loss of information due to interferences, noise pick-up and distortion by the transmission line.

As shown in Fig. 12, the analog front-end is connected to a reference resistor and an optional conductivity cell, in addition to the connections with the probes. The conductivity cell is used as a reference measurement in specific parts of the whole experimental apparatus, and is physically connected to the nearest sensor unit. Such conductivity cells perform a direct measurement of a liquid sample drained from any measuring section. The reference resistor input connects a high precision resistor to a generic measurement channel (identical to those used for the electrode probes), which is used as a reference channel. The high matching between identical channels in the front-end and the normalisation of the acquired measurements with respect to this reference channel, result in an improved immunity to drifts in the front-end electronics.

For what regards the analog signal processing chain shown in Fig. 12, the current signal is first converted to a voltage signal by a trans-impedance amplifier, based on a classical Operational Amplifier configuration. Such input stage provides the virtual earth reference mentioned earlier in this section. A second order high-pass and a smooth first order low-pass filter are respectively used to damp the mains supply noise and the radio-frequency noise picked-up by the cabling, forming a band-pass filtering, in the whole. The demodulator is synchronized with a delayed version of the excitation signal, in order to compensate for the phase shift due to the reactive component in the impedance of the probe-cabling-filter arrangement. After the final low-pass filtering, the signal is fed to the data acquisition board (A/D board), which provides digital conversion with a resolution of 16 bits, locally to each sensor unit.

All the sensor units share the same function generator, which provides a common source for the excitation signals used by all the probes (transmitting electrodes). The selected generator is characterised by a direct digital synthesis, ensuring an excellent stability and spectral purity of the generated sine-wave.

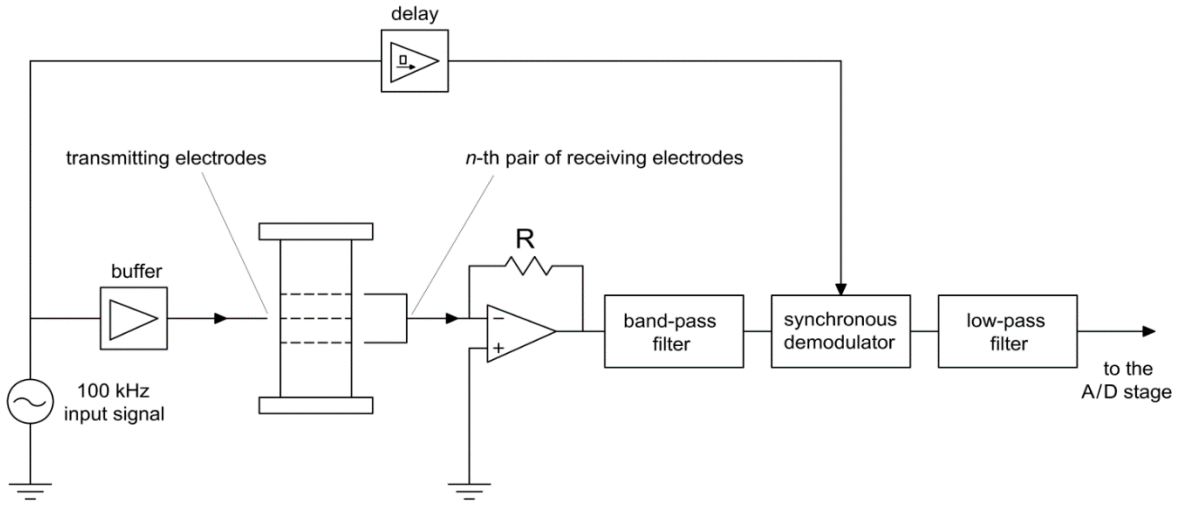

Fig. 12. Simplified structure of a measurement channel belonging to the analog front-end.

3.2 Data acquisition and display

A "Single Master-Multiple Slave" software architecture has been developed in order to monitor and acquire data at maximum speed, without having data loss and misalignment. The main functionalities implemented by the software can be summarized as follows:

- Real-time data acquisition. It is possible to monitor the overall system activity, access any sensor unit and manage every acquisition channel individually.
- Graphical User Interface and real-time data representation. Software architecture is split into an *Acquisition Control Program*, executed by the embedded-pc, and an *Administration and Monitoring Tool*, which displays data using graphical interfaces.
- Data storing and retrieving using a database interface. The *Monitoring Tool* handles communication with all the sensor units and stores data to a SQL database continuously.
- Online diagnostic tests capability.

The Administration and Monitoring Tool acts as a Single-Master and is executed on a dedicated workstation with multi-homed network configuration: one Gigabit Ethernet interface is dedicated to the communication with the multiple-slave set, another GBit Eth connects the workstation to local network for remote access. The communication module (DLL) implements data exchange using multiple sockets interfaces:

- UDP Server Socket for discovery operations and network topology self-arrangement.
- TCP Sockets for connection-oriented one-to-one communication with slaves; TCP ensures a reliable channel for data exchange with respect of the right flowing order for the data-communication messages.

The Acquisition Program runs on the embedded-PC and manages the low-level hardware interaction with High Performance A/D subsystem and the data dispatch to the workstation.

3.3 Signal processing

Acquired signals are voltage levels directly related to the measured conductance between each pair of electrical nodes, represented by one electrode belonging to the central array (transmitting electrode) and the two corresponding electrodes belonging to the side arrays (receiving electrodes), which are shorted together and sink the loop current that goes through the conducting liquid phase. As specified in Section 3.1, in order to limit the experimental errors, such signals are normalized with respect to a reference signal obtained by closing the current loop of a generic input channel with a reference resistor. This operation is performed by the data-collecting workstation, since it is preferred to transmit raw data from the local SBCs.

4. FLOW TEST

4.1 Free falling liquid layers

The study of free falling liquid layers in a circular duct has been chosen as preliminary application of the measuring section developed in the present work. The reason being that it represents the simplest case of stratified liquid flow in a pipe and is one of the few flow conditions which can be very well described with a semi-empirical method or by the numerical integration of Navier-Stokes equations. Analytical solutions of the Navier-Stokes equations for this flow condition are also available [28].

The semi-empirical method is based on the force balance

$$-\tau_{WL} S_L + \rho_L A_L g \sin\varphi = 0 \ , \tag{6}$$

where τ_{WL} is the shear stress at pipe wall, ρ_L the liquid density, g the gravity and φ the angle between the pipe and the horizontal. Taitel and Dukler [29] expressed τ_{WL} in terms of the friction factor f_L as

$$\tau_{WL} = \frac{1}{2} f_L \rho_L u_L^2 . \tag{7}$$

In this equation, u_L is the mean liquid velocity and f_L is assumed to be the same function of the liquid Reynolds number, Re_L, as in single phase flow, with Re_L defined as

$$\mathrm{Re}_L = \frac{4 A_L}{S_L} \frac{u_L}{\nu_L}, \tag{8}$$

where ν_L is the liquid kinematic viscosity. f_L can be predicted with the equations:

$$\mathrm{Re}_L \le 2000 \qquad f_L = \frac{16}{\mathrm{Re}_L}, \tag{9}$$

$$\mathrm{Re}_L > 2000 \qquad f_L = 0.046\, \mathrm{Re}_L^{-0.2} . \tag{10}$$

Andreussi and Persen [30] derived from Eq. (7) the following relation for the dimensionless liquid flow area, A_L^+:

$$A_L^+ = \frac{4 A_L}{S_L \nu_L} \left(\frac{\tau_{WL}}{\rho_L} \right)^{1/2} = \left(\frac{f_L}{2} \right)^{1/2} \mathrm{Re}_L . \tag{11}$$

According to this equation, A_L^+ is only a function of the liquid Reynolds number.

Giovine et al. [28] have shown that the analytical solutions of Navier-Stokes equations relative to single phase laminar flow in inclined pipes obtained for h/D = 0.5 and h/D → 0, almost coincide with the solution based on Eqs. (6)-(9). These authors also noticed that the numerical integration of N-S equations computed by Buffham [31] for laminar flow is very similar to the Taitel and Dukler solution for the entire range of liquid heights and concluded that the simplified approach to the problem reported above has a general validity for laminar flow conditions.

For turbulent flow, the Taitel and Dukler solution of the falling film problem is compared in Fig. 13 with the numerical integration of Navier-Stokes equations made with the VOF multiphase model of Fluent. In this computation the standard $k-\varepsilon$ model of turbulence has been used. As can be seen from Fig. 13, the simple solution of the falling film problem proposed by Taitel and Dukler [29] almost coincides with the results of the numerical integration also for turbulent flow, thus suggesting that in this simple case of stratified flow the theoretical predictions should be reliable.

In Fig. 12, the experimental measurements of Andreussi and Persen [30] and Lioumbas et al. [32] are also reported. As can be seen from this figure, for Re_L > 3000 the theoretical predictions provide a very good fit to the experimental measurements. For Re_L < 3000, the dispersion of the experimental measurements of Lioumbas et al. [32] is relevant. This may be due to the fact that at these Reynolds numbers the transition between laminar and turbulent flow occurs, but it is useful to recall that, on one hand, the relative error of film height measurements can be larger for thin rather than thick films; on the other hand, Lioumbas et al. [32] state in their paper that the estimated average uncertainty of their measurements is equal to 10%. At low Reynolds numbers, the scatter of the data shown in Fig. 13 is well above 20%.

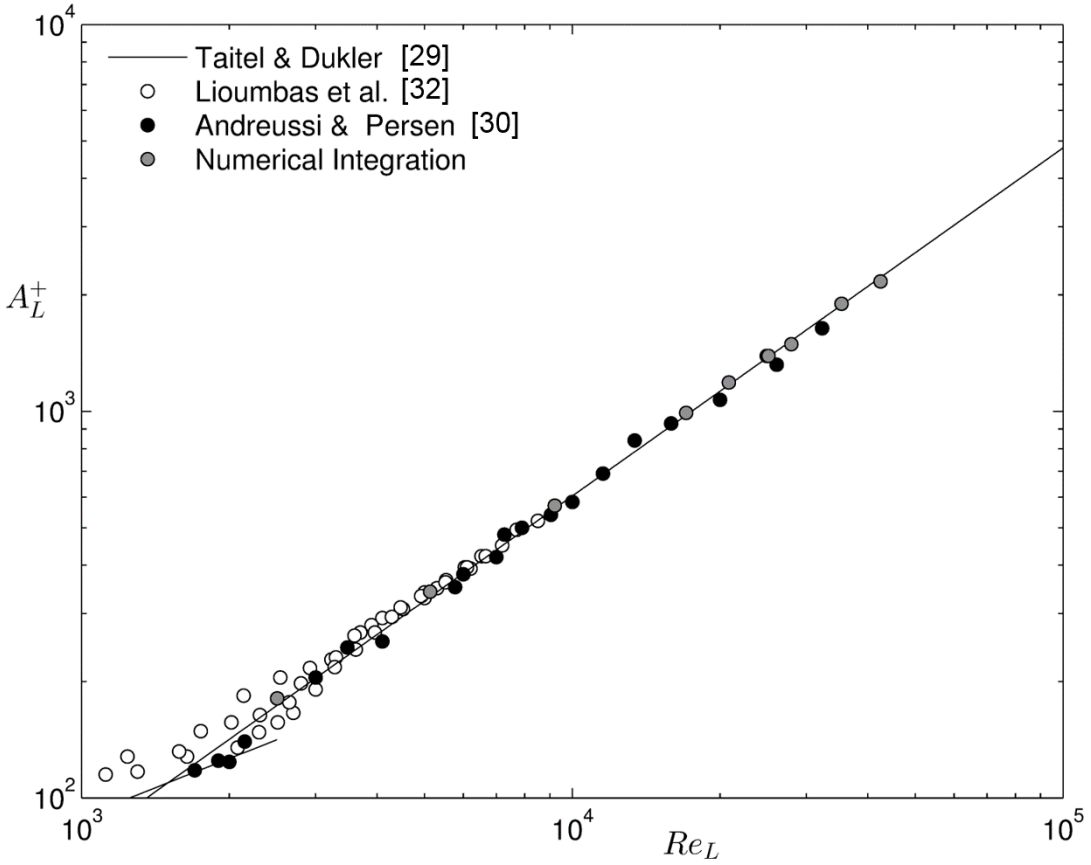

Fig. 13. Dimensionless liquid flow area vs liquid Reynolds number for a free falling liquid layer in a circular duct.

4.2 Experiments

The experiments have been conducted in the Multiphase Flow Laboratory of TEA Sistemi, a spin-off company of the University of Pisa. A simplified chart of the flow loop is shown in Fig. 7. The test section is approximately 10 m long and the pipe diameter is 80 mm. In present experiments the pipe is inclined on its support and its inclination with respect to the horizontal is carefully measured. This also requires the horizontal position of the test section to be identified. The final value of the pipe inclination can be determined with an overall accuracy which is estimated to be better than 0.04°. At the small inclinations investigated in the present work, this level of accuracy may generate an error of the order of 1-2% in the measurement of the film thickness. In the flow loop used by Andreussi and Persen [30], the pipe was 26 m long. This allowed a better measurement of its inclination, with an uncertainty estimated by these authors equal to 0.02°.

The working liquid is demineralized water whose conductance has been risen to values in the range 50-200 μS/cm by adding known amounts of KBr. The final conductivity and temperature of the water phase have been carefully measured and the expected uncertainty of conductance measurements is about equal to 2%. The overall accuracy of the present measurements is not expected to be better than 4%. Possibly most of the published film thickness measurements are affected by similar or larger uncertainties, as it appears from the work of Lioumbas et al. [32]. This level of uncertainty is partially related to the conductance method which requires an accurate measurement of the liquid conductivity.

4.3 Results and Discussion

The experimental measurements are relative to tests performed by two different operators who adopted different experimental procedures and set-ups. In particular, two methods have been used for probe calibration.

TEST A. The test section was assembled with 6 measuring sections and the vertical wire probes were calibrated simultaneously by closing both ends of the pipe and filling the pipe with different volumes of water. In this case the liquid level was only measured near each probe with the micrometric head described in Section 2.4. The micrometric head was also used to determine the horizontal position of the test section by measuring the liquid level at various positions along the section. It is useful to remark that it is very difficult to avoid minor misalignments (0.1-0.2 mm) among the different sections of the pipe. The liquid used for the calibration was the same liquid used for the tests. Its temperature was always carefully measured and the conductivity corrected for temperature variations both during the calibration and the tests. This procedure almost reduces to zero the error associated with the measurement of the liquid conductivity. The same procedure was followed by Andreussi and Persen [30].

TEST B. The test section was assembled with 3 measuring sections. Each measuring section was calibrated individually on the bench following the procedure described in Section 2.4. The section was filled with known volumes of water and the liquid height was also determined with the micrometric head. This procedure allows the calibration to be extremely accurate. In particular, any possible uncertainty about the inclination of the section with respect to the horizontal is reduced to zero because the probe is at the centre of the section. However, the liquid used for the calibration was not the same liquid used in the experiments and this leaves a possible source of error. The ring probe was also calibrated on the bench and used in this series of experiments.

The raw measurements are shown in Fig. 14, which reports the liquid height read with the central probe as a function of the liquid flow rate for three pipe inclinations. The multiple readings reported for each flow rate are relative to the 6 or 3 measuring sections used in tests A and B, respectively. In this figure it is reported that the dispersion of film height measurements is equal to 0.5 mm for test A and 1.0 mm for test B. This difference is due to the independent calibration performed for each probe in test B and provides an estimate of the uncertainty of the calibration procedure. From Fig. 14 it can be noted that the dispersion of the measurements appears to be independent from the film height, thus indicating that at low film heights the relative error of the measurements can be significant.

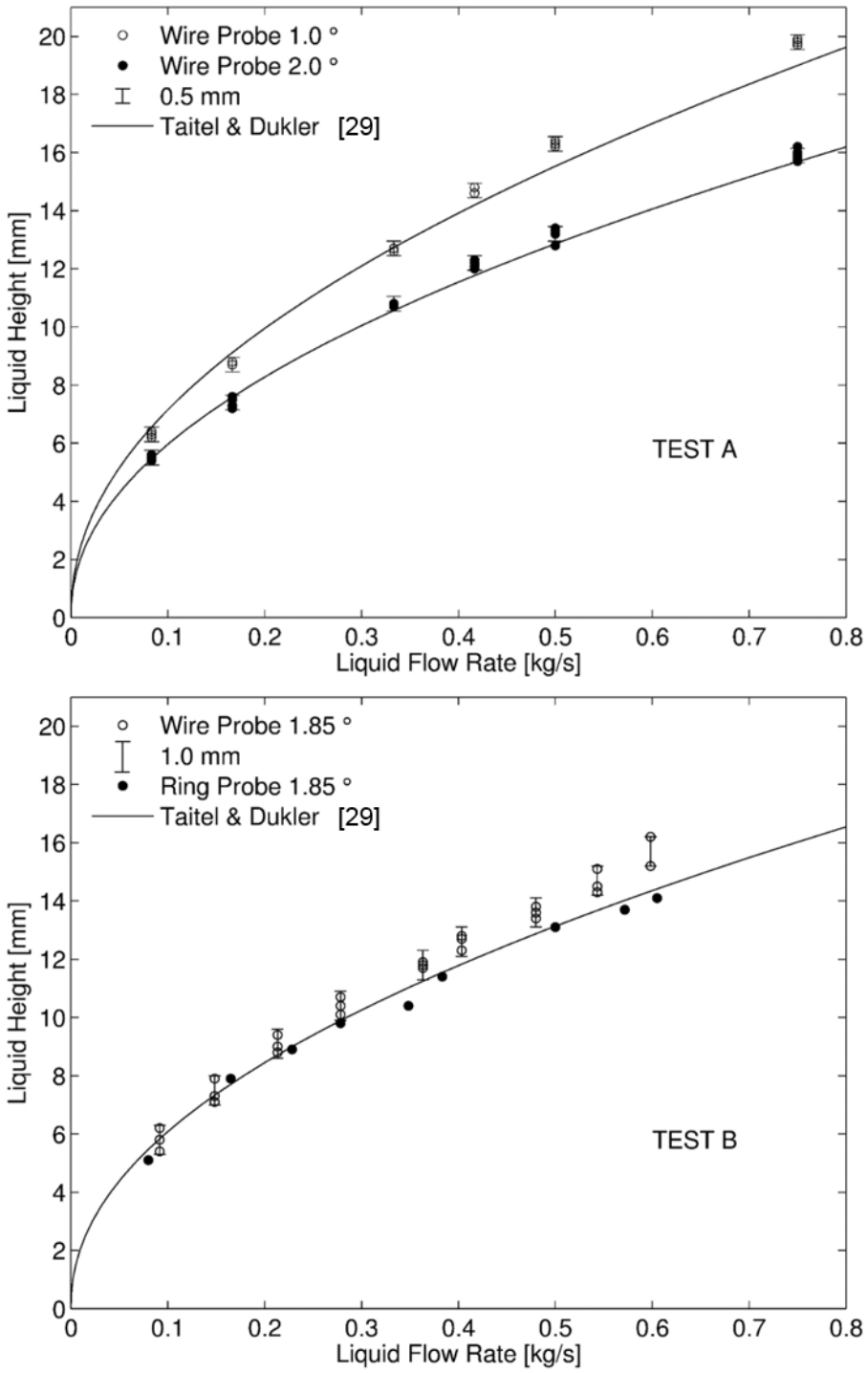

Fig. 14. Raw measurements for three pipe inclinations.

In Fig. 14, the hold-up measurements obtained with the ring probe and the theoretical predictions are also reported. The overall fit of the data is fairly good, in particular the ring probe data are only slightly below the predictions. The wire probe data appear to be affected by systematic, minor deviations in the range of large film heights. This difference is less than 4%, in case A and goes up to values about equal to 6% in case B. As the expected uncertainty of present measurements has been evaluated by taking into account only the results of the static probe calibration, the increased values of the experimental error can be attributed to the effects of the disturbances generated by wire probes at the gas-liquid interface. These disturbances are expected to increase at increasing liquid velocity, and of course do not regard the ring probe measurements.

5. CONCLUSIONS

A novel test section made of an array of conductance probes has been developed to study stratified and stratified-dispersed flow in horizontal or inclined pipes. The conductance probes provide fairly accurate readings of the circumferential film thickness distribution and, as shown by Pitton et al. [23], can also be used to determine the liquid film flow rate and the rates of droplet exchange by means of the tracer method [20]. Among the different probe geometries proposed in the literature, wire electrodes have been selected because they guarantee a linear response at varying the film thickness over a wide range.

The analytical or numerical integration of Laplace equation has been used to determine the probe conductance and optimize the geometry of the test section. The results obtained indicate that the theoretical predictions are quite accurate and agree very well with the static calibration of the probes. The integration of Laplace equation also allowed the dispersion of the electrical current toward the conducting parts of the pipe to be estimated with good accuracy. A new theoretical equation (Eq. 5) has been derived to predict the conductance of a three-wire probe immersed in an unbounded liquid layer.

The probe geometry is based on the use of three-electrodes spaced along the flow direction. This choice is related to the application of conductance probes to the measurement of the film thickness in metallic pipes, designed to operate at an appreciable pressure (40 Bar) and electrically connected to the earth potential. In the present application, the probes are installed in a non-conducting section of the pipe and the external electrodes of each probe are actively kept at the earth potential. This arrangement allowed the current dispersion to the external conductive components of the test rig to be minimized and substantially eliminates probe-to-probe interference. The three electrode configuration also enables the simultaneous operation of the 15 probes without multiplexing. The absence of multiplexing represents a noticeable advantage of the present set-up because it allows most of the demodulated signal bandwidth to be exploited and eliminates most sources of electrical switching noise and subsequent errors. In addition to enhancing signal integrity in the signal processing chain, this configuration binds the signals generated by the central array of wires into a limited volume of the liquid layer, providing a more localized measurement in the circumferential direction.

The disturbance generated at the gas-liquid interface by wire electrodes has been evaluated by the integration of Navier-Stokes equations using the Volume Of Fluid model. This disturbance can produce an error in the measurement of the film height about equal to 2% at the flow conditions examined in the present work. The magnitude of this error does not change significantly when comparing the present three wire configuration with the conventional one based on two wires.

The test section has been tested by measuring the height of free falling liquid layers in a circular duct. The semi-empirical solution proposed by Taitel and Dukler [29] has been compared with a 3-D flow simulation and a very good agreement has been found between these solutions of the problem. Published data agree with the predictions at large Reynolds numbers, but the scatter of measurements is significant at low film heights, in a range of liquid Reynolds numbers corresponding to the transition between laminar and turbulent flow. For this case the experiments reported by Lioumbas et al. [32] are affected by deviations from the theoretical predictions greater than 20%, probably due to experimental errors. Also present measurements are affected by systematic, low deviations from the theoretical predictions. The magnitude of these deviations is quite small for ring probes and more significant for wire probes. It seems possible that the scatter of present measurements be related to the measurement of the electrical conductivity, minor errors affecting the pipe inclination and, finally, for the case of wire probes, the disturbances generated by the probes at the gas-liquid interface.

References

[1] Bonizzi M, Andreussi P, Banerjee S. Flow regime independent, high resolution multi-field modelling of near-horizontal gas–liquid flows in pipelines. Int. J. Multiphase Flow 2009;35:34-46.

[2] Miya M, Woodmansee DE, Hanratty TJ. A model for roll waves in gas-liquid flow. Chemical Engineering Science 1971;26(11):1915-1931.

[3] Brown RC, Andreussi P, Zanelli S. The use of wire probes for the measurement of liquid film thickness in annular gas-liquid flows. Can. J. of Chem. Eng. 1978;56(6):754–757.

[4] Coney MWE. The theory and application of conductance probes for the measurement of liquid film thickness in two-phase flow. J. Phys. E: Scient. Instrum. 1973;6:903-910.

[5] Asali JC, Hanratty TJ, Andreussi P. Interfacial drag and film height for vertical annular flow. AIChE J. 1985;31:895–902.

[6] Geraci G, Azzopardi BJ, van Maanen HRE. Effect of inclination on circumferential film thickness variation in annular gas/liquid flow. Chem. Eng. Sci. 2007;62:3032-3042.

[7] Nydal OJ, Pintus S, Andreussi P. Statistical Characterization of Slug Flow. Int. J. Multiphase Flow 1992;18:439-453.

[8] Zhao Y, Markides CN, Matar OK, Hewitt GF. Disturbance wave development in two-phase gas–liquid upwards vertical annular flow Int. J. Multiphase Flow 2013;55:111-129.

[9] Andreussi P, Di Donfrancesco A, Messia M. An Impedance Method for the Measurement of Liquid Hold-up in Two-Phase Flow. Int. J. Multiphase Flow 1988;14:777-785.

[10] Fossa M. Design and performance of a conductance probe for measuring the liquid fraction in two-phase gas-liquid flows. Flow Meas. and Instrum. 1998;9:103–109.

[11] Barral AH, Angeli P. Spectral density analysis of the interface in stratified oil–water flows. Int. J. Multiphase Flow 2014;65:117–126.

[12] Prasser H-M, Böttger A, Zschau J. A new electrode-mesh tomograph for gas–liquid flows. Flow Meas. and Instrum. 1998;9:111–119.

[13] Vieira RE, Kesana NR, Torres CF, McLaury BS, Shirazi SA, Schleicher E, Hampel U. Experimental Investigation of Horizontal Gas–Liquid Stratified and Annular Flow Using Wire-Mesh Sensor. Journal of Fluids Engineering 2014;136(12):1-16.
[14] Damsohn M, Prasser H-M. High-speed liquid film sensor for two-phase flows with high spatial resolution based on electrical conductance. Flow Meas. and Instrum. 2009;20:1–14.
[15] Tiwari R, Damsohn M, Prasser H-M, Wymann D, Gossweiler C. Multi-range sensors for the measurement of liquid film thickness distributions based on electrical conductance. Flow Meas. and Instrum. 2014;40:124-132.
[16] Paras SV, Karabelas AJ. Properties of the liquid layer in horizontal annular flow. Int. J. Multiphase Flow 1991;6(1–2):439–54.
[17] Bieberle A, Hoppe D, Schleicher E, Hampel U. Void measurement using high-resolution gamma-ray computed tomography. Nuclear Eng. and Design 2011;241(6):2086-2092.
[18] Zhang Z, Bieberle M, Barthel F, Szalinski L, Hampel U. Investigation of upward concurrent gas-liquid pipe flow using ultrafast X-ray tomography and wire-mesh sensor. Flow Meas. And Instr. 2013;32:111-118.
[19] Schubring D, Ashwood AC, Shedd TA, Hurlburt ET. Planar laser-induced fluorescence (PLIF) measurements of liquid film thickness in annular flow. Part I: Methods and data. Int. J. Multiphase Flow 2010;36(10):815-824.
[20] Quandt ER. Measurement of Some Basic Parameters in Two-Phase Annular Flow. AIChE J. 1965;11:311-318.
[21] Andreussi P. Droplet Transfer in Two-Phase Annular Flow. Int. J. Multiphase Flow 1983;9:697-713.
[22] Schadel SA, Leman GW, Binder JL, Hanratty TJ. Rates of atomization and deposition in vertical annular flow. Int. J. Multiphase Flow 1990;16(3):363-374.
[23] Pitton E, Ciandri P, Margarone M, Andreussi P. An experimental study of stratified-dispersed flow in horizontal pipes. Int. J. Multiphase Flow 2014;67:92-103.
[24] Ito D, Prasser H-M, Kikura H, Aritomi M. Uncertainty and intrusiveness of three-layer wire-mesh sensor. Flow Meas. and Instrum. 2011;22:249–256.
[25] Kim J, Ahn Y-C, Kim MH. Measurement of void fraction and bubble speed of slug flow with three-ring conductance probes. Flow Meas. and Instrum. 2009;20:103-109.
[26] Ritcher S, Aritomi M, Prasser H-M, Hampel R. Approach towards spatial phase reconstruction in transient bubbly flow using wire-mesh sensor. Int. J. Heat Mass Transfer 2002;45:1063–1075.
[27] Devia F, Fossa M. Design and optimisation of impedance probes for void fraction measurements. Flow Meas. and Instr. 2003;14:139–149.
[28] Giovine P, Minervini A, Andreussi P. Stability of liquid flow down an inclined tube. Int. J. Multiphase Flow 1991;17(4):485-496.
[29] Taitel Y, Dukler AE. A model for predicting flow regime transitions in horizontal and near Andreussi horizontal gas-liquid flow. AIChE J. 1976;22:47-55.
[30] Andreussi P, Persen LN. Stratified Gas-Liquid Flow in Downwardly Inclined Pipes. Int. J. Multiphase Flow 1987;13(4):565-575.
[31] Buffham BA. Laminar flow in open circular channels and symmetrical lenticular tubes. Trans. Inst. Chem. Engrs 1968;46,T153.
[32] Lioumbas JS, Paras SV, Karabelas AJ. Co-current stratified gas–liquid downflow —Influence of the liquid flow field on interfacial structure. Int. J. Multiphase Flow 2005;31:869–896.

Acknowledgements

The Financial contribution of ENI E&P and TEA Sistemi spa is gratefully acknowledged. E. Pitton wishes to acknowledge the advice and support of Marina Campolo of the University of Udine.